COMPEL - The international journal for computation and mathematics in electrical and electronic engineering

A statistical study of scattering in periodic and random helix layers

Christian Meiners, Arne F. Jacob,

A statistical study of scattering in periodic and random helix layers

Christian Meiners
Ritz Instrument Transformers GmbH, Hamburg, Germany, and
Arne F. Jacob
Institut für Hochfrequenztechnik, Technische Universität Hamburg-Harburg, Hamburg, Germany

Abstract

Purpose – This paper aims at providing information on scattering in layers composed of periodic and non-periodic arrangements of small metal helices. Metal helices exhibit a pronounced resonance and are thus very effective scatterers.

Design/methodology/approach – Scattering is expressed in terms of multipole moments. Non-periodic layers are investigated using the combination of periodic boundary conditions for sample configurations and averaging many of these configurations. The results and the methodology are compared to the well-known Clausius-Mossotti (CM) mixing rule and the assumptions and concepts therein. This is done to deepen the understanding of the scattering behavior.

Findings – The investigations show that only few multipole contributions are necessary to model the interaction correctly.

Originality/value – A systematic comparison of a full-wave scattering theory and the fast CM mixing theory is conducted, providing some physical insight. From this, conclusions on the validity of the mixing approach are drawn.

Keywords Metals, Composite materials

Paper type Research paper

1. Introduction

In this contribution, composite materials consisting of small metal helices are investigated. This type of inclusion is known from artificial chiral materials in the microwave domain, which attracts interest since the early 1990s (Lindell *et al.*, 1994). While the geometric dimensions are small compared to the wavelength, it is an effective scatterer at resonance. For this reason, metal helices can be used, e.g. to improve microwave absorbers at the lower frequencies. In order to model such materials, full-wave methods and analytical mixing rules have been applied (Whites, 1995; Guérin *et al.*, 1995). The disadvantage of the proposed approaches is that the mechanisms of mutual couplings can usually not be identified. This prevents the growths of a deeper understanding of such materials.

Here, for a detailed analysis of the scattering mechanisms, a complete multipole model of a single helix is applied. The latter is based on the T-matrix, which relates the complex amplitudes of the incoming and scattered waves both expanded into vector spherical harmonics. Once periodic boundaries are implemented, the scattering parameters of 2D-infinite and regular layers can be calculated.

The authors wish to thank the DFG (Deutsche Forschungsgemeinschaft) for financial support.

COMPEL: The International Journal for Computation and Mathematics in Electrical and Electronic Engineering
Vol. 30 No. 4, 2011
pp. 1162-1175

0332-1649
DOI 10.1108/03321641111133109

Layers with more statistics are modeled by an averaging approach (Figure 1): the results of several periodic layers are summed up and later on divided by the number of calculated configurations. Thereby, a unit cell of each periodic configuration contains several helices, which are positioned and oriented according to a given statistical distribution. The convergence of the method is checked with respect to the number of required configurations and helices per unit cell. Afterwards, the transition from a 2D-periodic to a random layer is carried out in steps in order to cover a wide range of constellations in a systematic manner. Here, also the role of the different multipole moments in the interaction process is addressed. The full-wave scattering theory is used to check the validity range of the widely used Clausius-Mossotti (CM) mixing theory.

2. Multipole model

The T-matrix of the helix is calculated according to the procedure outlined in Meiners *et al.* (2008). Thereby, the caused current on the helix (due to the excitation) is divided into elementary dipoles. The scattered fields of the latter are expressed by first-order vector spherical harmonics with respect to the origin of each dipole element. Subsequently, these fields are re-expanded to obtain a common origin for all waves, i.e. the origin of the helix. This algebraic expansion automatically accounts for higher order multipoles since the order of the arising spherical waves increases. The current on the helix is calculated separately for each incoming spherical wave. In this way, the T-matrix is obtained column wise.

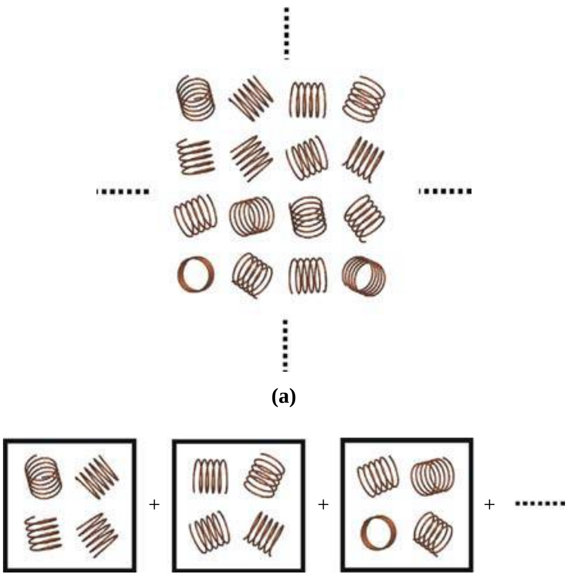

(b)

Notes: (a) Random layer; (b) similar problem with reduced complexity

Figure 1. Illustration of the averaging method

The type of helix considered in this paper is specified by Table I.

It turns out, that the resonance frequency of such a helix is $f_{res} \approx 4.96\,\text{GHz}$.

The implementation of periodic boundaries is not presented in this paper. Details can be found in Meiners *et al.* (2008).

3. Convergence

An example of how to control the kind of randomness within a layer is shown in Figure 2.

The helices are located on a rectangular grid and their orientations are varied – here, with respect to the y-axis in the xy-plane. The maximum admissible deviation from the original (periodic) orientation is denoted by the parameter ψ. Thereby, a random number calculator (uniform distribution) is used to determine the actual orientation of each helix within the layer or the unit cell, respectively.

The investigations in Meiners *et al.* (2008) show that the helices have to be very close to each other before higher order multipole effects become noticeable. Here, we choose a lattice constant of 3 mm. As will be also demonstrated later, multipoles of up to third order thus may contribute to mutual coupling. For this reason, the simulation always includes dipoles, quadrupoles and octupoles if not stated otherwise.

Table I.
Geometry of the investigated helix

No. of turns	5, right turned
Radius	0.8525 mm
Pitch	0.35 mm
Wire length	26.84 mm
Electrical conductivity	11 MS/m

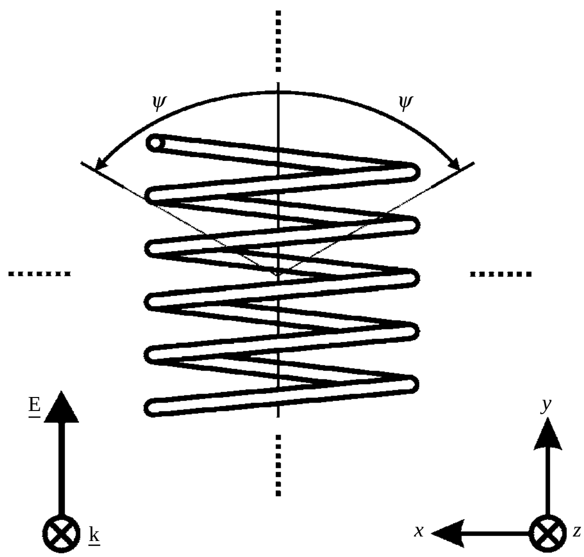

Figure 2.
Investigated rotation

Figure 3 shows the co-polarized scattering parameters (the cross-polarized parameters show similar behavior and have been omitted here). This investigation has been conducted for 25 helices in the unit cell (5 × 5 case) and $\psi = 45°$. The frequency is set to $f = 4.6$ GHz which corresponds to the resonance of the layer. As can be seen, the scattering parameters do not change much for many (>2,500) configurations. On the other hand, few calculations in the order of 100 are sufficient for a relative deviation of 1-2 per cent. Due to the non-regular convergence, it is generally not possible to interpolate. In this contribution, convergence is assumed if all the scattering parameters of the last 100 configurations deviate by $<10^{-3}$ from the average value. In terms of the present investigation, convergence is achieved for 528 calculated configurations. This leads to a relative deviation of <0.5 per cent with respect to the case of 3,000 configurations.

Concerning the magnitude of the scattering parameters, the resonance of the layer at $f = 4.6$ GHz is the most interesting case. For a further assessment of the solution, the number of helices per unit cell is considered while the grid is kept constant. The results are shown in Figure 4.

From approximately 49 helices (7 × 7) on, the influence of the cell size reduces. Compared to the 11 × 11 case, deviations of only 0.5 dB occur. Due to the pronounced

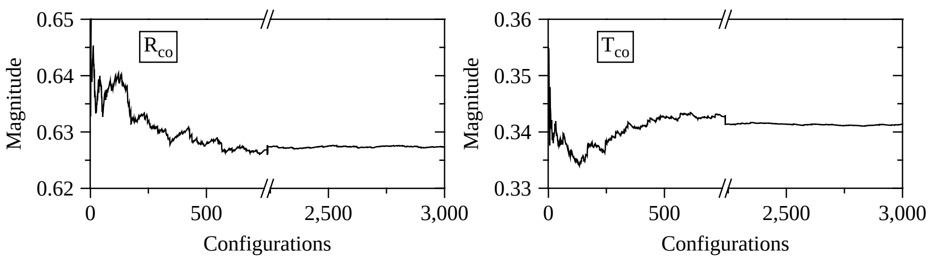

Figure 3. Magnitude of the co-polarized reflection and transmission as a function of calculated configurations ($f = 4.6$ GHz)

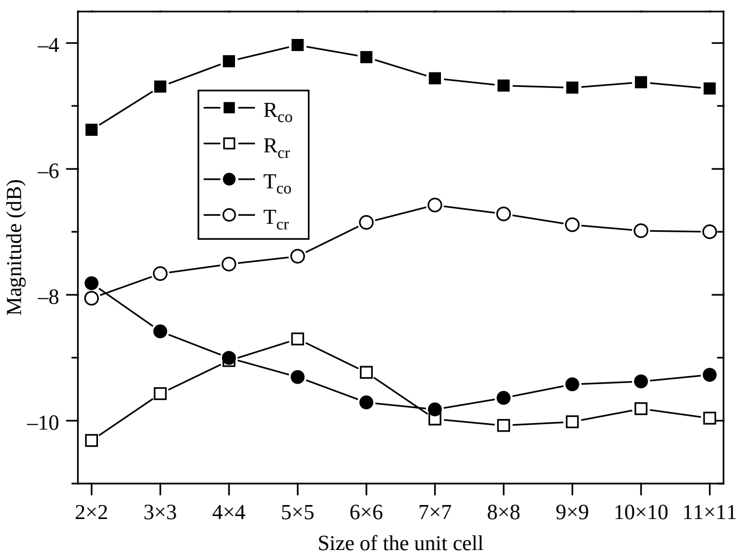

Figure 4. Magnitude of scattering parameters as a function of the cell size ($\psi = 45°$)

scattering behavior at resonance, this study renders a worst-case scenario. A faster and more regular convergence has been observed for frequencies well below or above the first resonance.

Figure 5 shows the cell size versus the required CPU-time and the number of configurations. The latter rapidly drops from above 1,000 to about 400. However, the progression is not regular which as well results from considering the resonance case. In order to yield a more comprehensive conclusion, also the average number of configurations for 91 equispaced frequency points in the frequency range from 4.0 to 5.8 GHz is shown. The smooth behavior as well as the very gentle slope for more than 36 helices per unit cell indicates that a satisfactory convergence is achieved. Further increasing the cell size does not necessarily lead to a much better representation of the statistical parameters. Anyway, concerning the rapidly growing CPU-time of, e.g. nearly 13 hours for 121 helices (one frequency point), a compromise between accuracy and suitability has to be found. The results presented in the following section have been obtained for 49 helices per unit cell. Here, it also has to be remarked, that usually the number of configurations is lower for both larger and smaller values of ψ. In this sense, the considered case $\psi = 45°$ represents a worst-case scenario.

4. Transition from periodicity to randomness

This section contains a study on the effects of different grades of variations. To this end, the parameter ψ is raised in steps of $\psi = 15°$ starting from $\psi = 0°$ (periodic case).

4.1 Scattering parameters

The obtained set of curves for the scattering parameters is shown in Figure 6. It can be seen that, compared to the periodic case, the scattering parameters do not change much for small variations ($\psi = 15°$). This behavior can be traced back to the fact that the strength of the external excitation for a single helix depends on the cosine of the angle between helix axis and the field vector of the incident wave. For this reason,

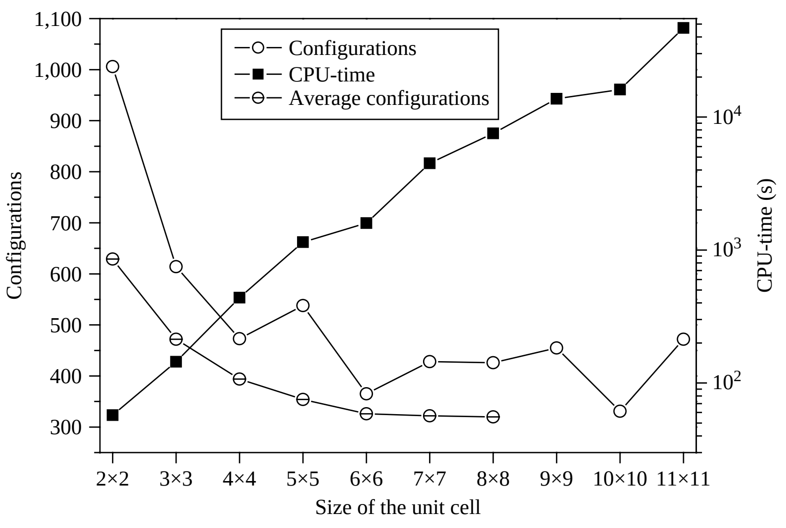

Figure 5.
Required number of configurations and CPU-time (standard PC, single core, 3 GHz clock rate) for different cell sizes

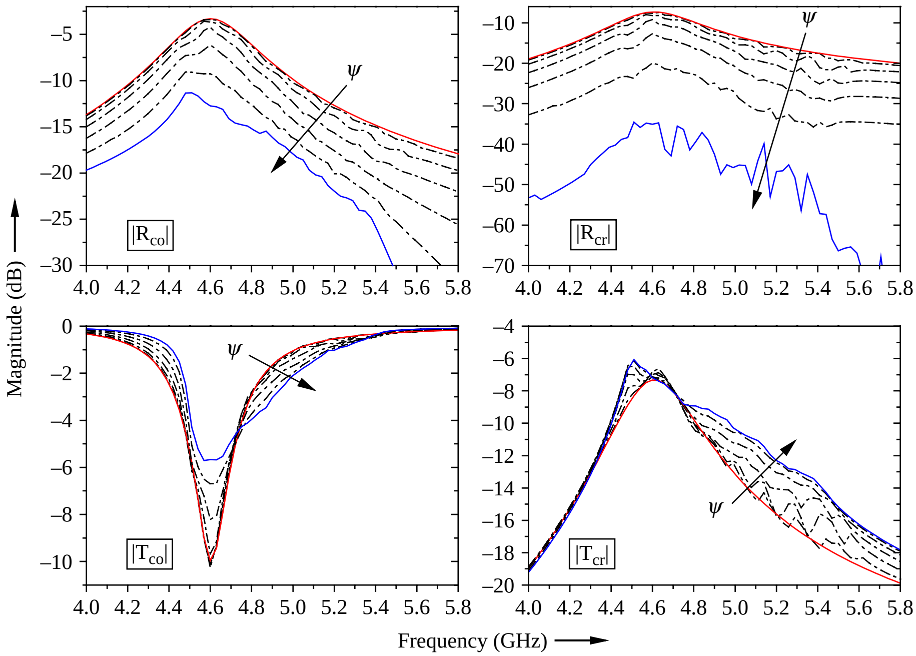

Note: Solid lines: $\psi = 0°$ and $\psi = 90°$, dashed lines: $\psi = i.15°$ with i = 1, . . . ,5

Figure 6.
Rotations of the helix axis according to Figure 2: influence of the parameter ψ on the scattering parameters of the layer

likewise the co-polarized reflection decreases with increasing ψ, while the co-polarized transmission grows. It is especially interesting that the cross-polarized reflection drops to -35 dB and below. This characteristic is very similar to the vanishing cross-polarized reflection for a bi-isotropic (chiral) medium.

The following considerations help understanding the curve progression for the cross-polarized components shown in Figure 6. The cross-polarized components of the far-field mainly stem from a combination of an electric ($p_x^e \underline{\mathbf{e}}_x$) and a magnetic dipole moment ($p_y^m \underline{\mathbf{e}}_y$). Here, the vector $\underline{\mathbf{e}}$ denotes the unit vector of the corresponding coordinate. The evoked plane waves superpose differently in the two half-spaces separated by the layer. Therefore, the cross-polarized reflection usually differs from the cross-polarized transmission. For the periodic case, they are nearly equal which is somehow masked in the figure due to the different scaling. But, this can only be the case if one dipole moment dominates the other. Actually, the amplitude of the wave stemming from the magnetic dipole moment is three orders of magnitude larger than that from $p_x^e \underline{\mathbf{e}}_x$. If the layer as a whole is rotated by 90° and if the excitation is kept constant, the dual case occurs. Apparently, for $\psi = 90°$ the effects of both dipole moments add up such that the cross-polarized reflection is nearly suppressed.

Here, it has to be remarked, that for $\psi = 90°$ merely the axis of the helix is randomly orientated in the xy-plane. Since a helix is not symmetrical with respect to its axis, entire randomness is only obtained for $\psi = 180°$. Alternatively, this goal could be accomplished by $\psi = 90°$ and additional (randomly) chosen rotations of 180° with respect to the helix axis. Further studies show that the influence of the latter type of rotation on the scattering parameters is very low. For this reason, one can consider $\psi = 90°$ as the case of nearly entire randomness in terms of rotations in the xy-plane. Of course, other types of orientations and also deviations of the position could be investigated.

4.2 Multipoles

The previously shown scattering parameters have been obtained by considering multipoles of up to third order. Concerning the spacing of the helices, this is always sufficient for a precise solution (Meiners *et al.*, 2008). However, so far the influence of the different contributions has not been investigated. To this end, the results are opposed to those obtained by taking only dipole contributions into account. As an example, the curves of the co-polarized reflection are shown by Figure 7.

In the periodic case, the two solutions mainly differ in terms of the resonance frequency. Here, a frequency shift of about 150 MHz is visible. This corresponds to a relative error of approximately 3.3 per cent. For increased variations, the curves more and more conform to each other. An interpretation is given in the following. For the periodic layer, the errors that are made in the description of the mutual couplings obviously add up. On the other hand, they tend to average out for random layers. This effect becomes more pronounced with increasing randomness. This was verified by means of several other investigated types of variations. Two more points are worth mentioning:

(1) as has also been found in Meiners *et al.* (2008) for a different layer setup, the quadrupoles have only little influence on the solution; and

(2) it is remarkable that, although an error is present in the dipole case, the conservation of energy is never violated.

5. Mixing rule

Multilayered helix arrangements are analyzed next. Without loss of generality, only racemic layers, that is, with equal number of left- and right-turned helices are considered.

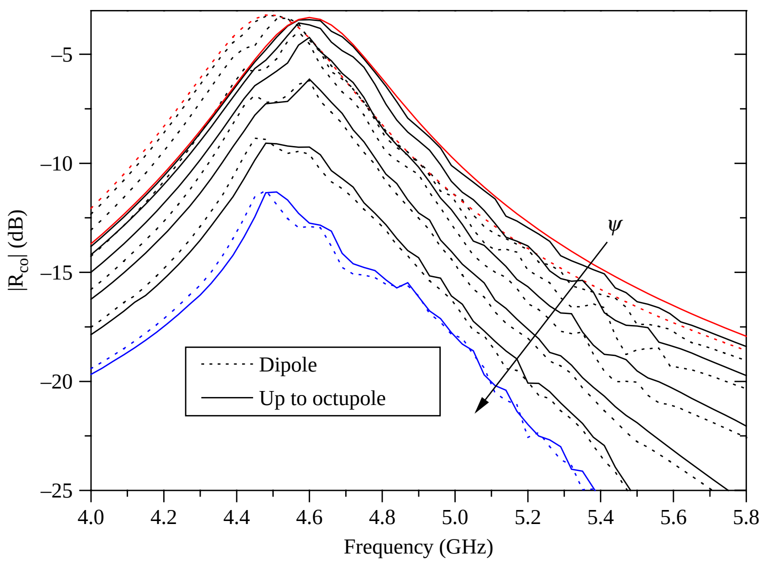

Figure 7.
Rotations of the helix axis according to Figure 2: influence of the parameter ψ on the co-polarized reflection

This is motivated by the reduced amount of data to be processed – a consequence of the missing cross-polar component. A simple example is considered first. For the sake of conciseness, the discussion of the scattering mechanism is kept shorter than above.

A multilayered structure of sufficient thickness and with a large number of small inclusions can reasonably be assumed to be homogeneous. Its equivalent material parameters could, for instance, be calculated from its inverted scattering parameters (Chen *et al.*, 2004; Smith *et al.*, 2002). In contrast, the effective material parameters are obtained from mixing formulas. The following is devoted to the question, whether this approach is suited to describe composite multilayers. To this end, the CM theory is applied to a three-layer helix arrangement. The comparison of the two approaches is conducted based on the scattering parameters instead of the material parameters. This simplifies the physical interpretation of the differences and their consequences.

The effective media theory as formulated by Clausius and Mossotti is only briefly sketched here, since comprehensive representations can be found in the literature (Sihvola, 1999). The theory provides a simple analytical formulation for the effective material parameters of a general bianisotropic medium. Only the properties of the host medium and the density as well as the average dipole polarizabilities of the inclusions are needed. Averaging possibly has to take into account different types of inclusions, their respective density – this is referred to as multiphase mixture – and their orientation. In this work, the averages are obtained from the scattering approach described above, as it already provides a statistically relevant number of different T-matrices. From the latter, the average T-matrix can be calculated, a 36-element sub-matrix of which yields the averaged dipole polarizabilities. An important aspect arises from this. Both the T-matrix and the dipole polarizabilities are defined with respect to the origin of the respective inclusion. However, as discussed above, the spatial distribution of the particles – and not only their density – might affect the scattering parameters. This is different for the mixing theory, which justifies the following investigations.

Figure 8 shows a detail of the analyzed three-layer setup of left- and right-turned helices. The particles are arranged on a $D = 6$ mm grid. This larger value accounts for the expectation that CM theory performs better in low-density materials.

The effective material parameters of a racemic medium are the permittivity and permeability. Because of the considered anisotropy, these are tensor quantities, though. Incase the helices are essentially aligned with one of the Cartesian coordinates the tensors are diagonal in good approximation. Their elements are different, in general, which reflects the direction and polarization dependent properties of the anisotropic material. Random orientation of the inclusions yields:

$$\varepsilon_{xx} = \varepsilon_{yy} = \varepsilon_{zz} \text{ and } \mu_{xx} = \mu_{yy} = \mu_{zz},$$

that is, a description of the isotropic medium by means of scalars.

Once the effective material parameters have been determined, the reflection and transmission coefficients can be calculated from the boundary conditions at the layer interfaces for a given layer thickness. A mathematical derivation can be found in Berremann (1972).

5.1 Comparisons for periodic layers

A critical issue is the definition of the layer thickness. A slab with a very large number of layers is not problematic in this respect, since it is orders of magnitude thicker than the

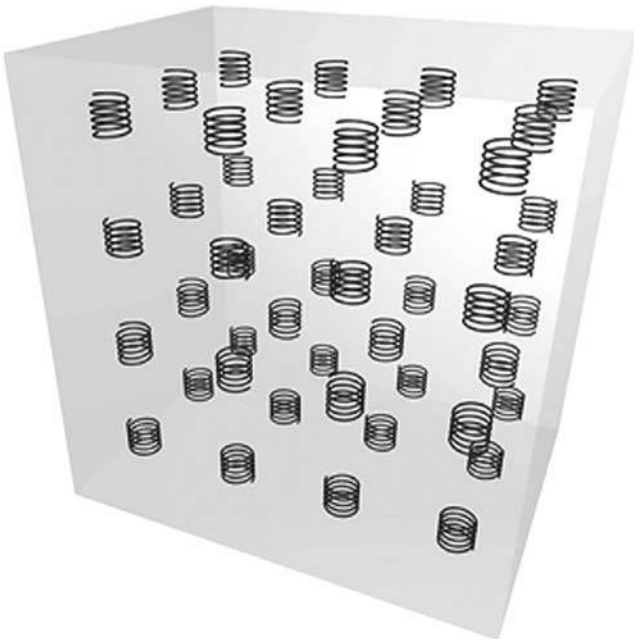
Note: Here with lattice constant $D = 6$ mm

Figure 8. Detail of periodic layer arrangement. The left and right turned helices are placed on a regular grid

diameter of the inclusions – in contrast to very thin layers, as considered in this work. The problem has already been addressed in Meiners and Jacob (2008) for thin layers of randomly positioned and oriented particles. Strongly varying particle couplings (resonance splitting) do not allow generalizing the results of Meiners and Jacob (2008). This is why these investigations are repeated here for periodic arrangements.

Figure 9 shows the calculated scattering parameters for the multilayer of Figure 8 at normal incidence. The electric field vector is parallel to the helix axis. In case of CM simulation, the layer thickness d is varied in steps of 1 mm, the density being adjusted accordingly. The transmission, especially around resonance, exhibits strong variations, partly exceeding 10 dB. These deviations occur at a low level, though.

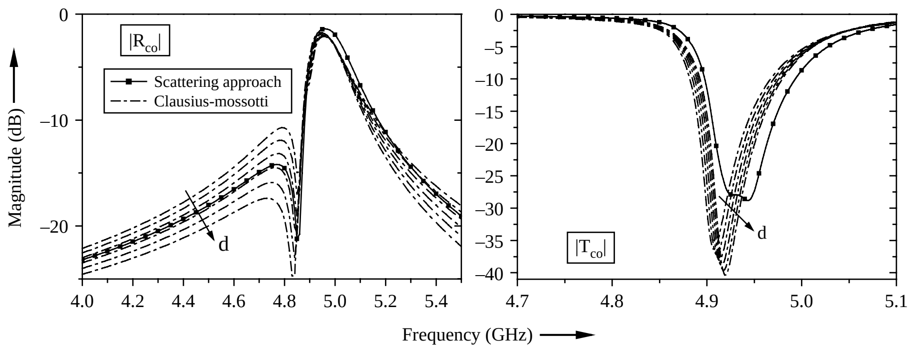

Figure 9. Normal incidence scattering parameters for different layer thicknesses ($d = 15$, 16, 17, 18, 19, 20 mm) in the CM model in comparison to the scattering theory ($\psi = 0°$)

Depending on the value of d, the agreement between the two approaches is better either regarding the dispersion characteristic or the scattering amplitude. In the following, we use:

$$\delta = \frac{1}{N_F} \sum_{i=1}^{N_F} \left(\left| R_{co,sca} \right| - \left| R_{co,CM} \right| \right)^2 + \left(\left| T_{co,sca} \right| - \left| T_{co,CM} \right| \right)^2$$

as a global measure for the deviation. The subscript *co* refers to co-polarization, the other ones are self-explanatory. The N_F frequency points are spaced by 10 MHz and distributed over the whole frequency range shown in Figure 9. The smallest deviation occurs at $d = 18$ mm, which reflects the $D = 6$ mm grid of the three-layer arrangement. Although this minimum was determined in a rather crude and not very general way, this result (which could have been anticipated) shows that CM theory can reasonably be applied to periodic helix arrangements at normal incidence. The good agreement of the reflection coefficient is to be noted.

The dependence of δ on the angle of incidence is shown in Figure 10.

For comparison, the results for several thickness values are included. Except for very obtuse angles beyond approximately 80°, the deviation increases strongly in the transverse electric (TE) case, as opposed to the transverse magnetic (TM) case, where the variations are much less pronounced. This correlates with the excitation strength of each helix, which is to a great extent governed by the angle between helix axis and electric field vector. In the TM case, it increases with the angle of incidence. Obviously, this is beneficial for the agreement between the two theories over a wider angular range. It is further noticeable that around 60°, the deviation δ even becomes smaller with increasing layer thickness d. This additionally hints at the difficulty of precisely defining the latter.

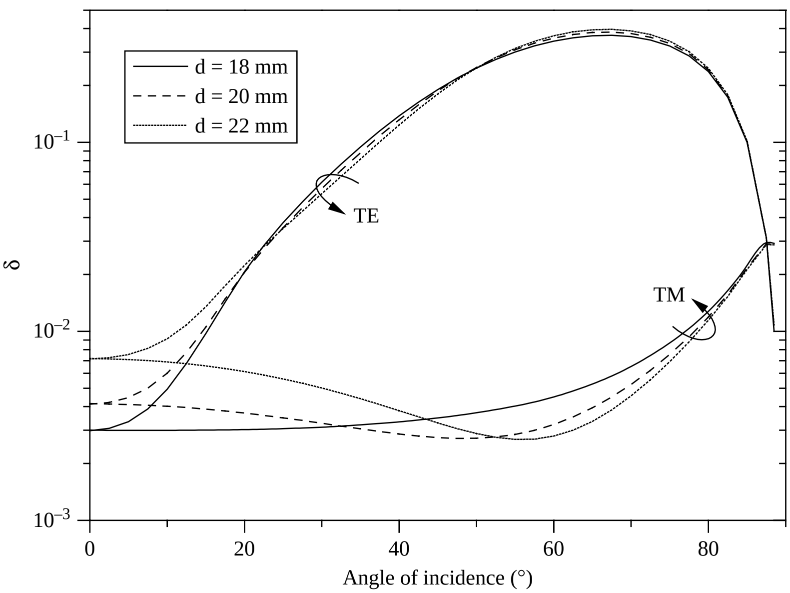

Figure 10.
Reflection coefficient for different layer thicknesses in the Clausius-Mossotti model in comparison to the scattering approach ($\psi = 0°$)

In the following, the density of the inclusions is varied by altering the lattice constant. According to the findings above, the layer thickness is hereby assumed to be three times that value. The calculated reflection coefficient is shown in Figure 11.

For the sake of conciseness, the spectra of the transmission coefficient are omitted here.

The case of very closely spaced particles ($D = 3$ mm) with resulting strong mutual coupling exhibits a pronouncedly different resonant frequency, as Figure 11 shows. When higher order moments (up to octupoles) are required for accurate results the dipole based CM theory clearly has weaknesses. This is supported by corresponding results of the scattering approach obtained with only dipole moments. These findings in principle also apply to the transmission behavior. The dependencies are partly quite different, though, especially at the transmission minima.

5.2 Comparisons for random layers

In the following, the applicability of CM theory is studied for layers exhibiting some disorder. The starting point is a periodic arrangement with $D = 4$ mm for which both approaches show a reasonable agreement, at least regarding the reflection coefficient.

Figure 12 compares the scattering parameters of a layer with a strictly periodic particle placement, a slightly disordered arrangement, and a purely random distribution. Here, d_m denotes the average distance between adjacent inclusions in a cell and ψ_p the maximum deviation between nominal and actual particle position in case of random distribution. The latter are determined numerically by "shuffling" the arrangement like in the procedure outlined in Ding *et al.* (1992). Most noticeably, the reflection coefficient calculated from CM theory exhibits several resonances in the vicinity of its maximum for increased randomness. At the same time, the difference between the transmission coefficients as obtained from the two approaches increases. The scattering approach yields a much broader and less pronounced response at resonance. For the random layer,

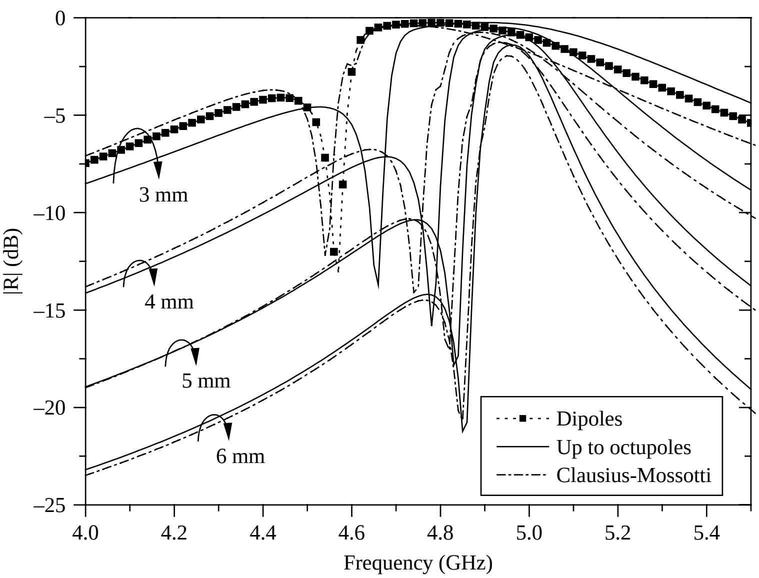

Figure 11.
Normal incidence reflection coefficient of periodic three-layer arrangement for different lattice constants D. Comparison of CM theory and scattering approach

the difference amounts to more than 45 dB. This clearly reflects the limitations of CM theory, which assumes that all particles interact in the same manner with their environment. More specifically, the varying degree of mutual coupling implies a multitude of resonances at different frequencies. Their superposition determines the behavior of the whole layer, the resonance of which thus exhibits a reduced quality factor. Further, by placing such a layer in front of a metallic screen, the poor agreement remains (Meiners and Jacob, 2006, 2008). From this, it can be concluded that for many structures consisting of the considered helices CM theory is inappropriate or may only be applied for a first estimation of the properties.

Nonetheless, one can retain from the above findings that CM theory also has its strengths, namely when the particles:

- are homogeneously distributed; and
- couple only weakly as, for instance, in low density materials.

To elaborate this last point, the case of a random layer issued from the above periodic arrangement with $D = 4$ mm shall be considered. For reduced coupling, the helices are centred in embedding spheres of 3 mm diameter and consisting of a lossy dielectric material. Figure 13 shows the results.

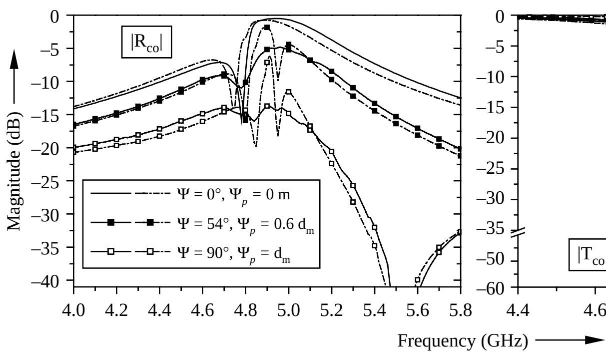

Note: Solid line: scattering approach, dashed-dotted line: CM theory

Figure 12.
Scattering parameters for $D = 4$ mm and different degrees of randomness

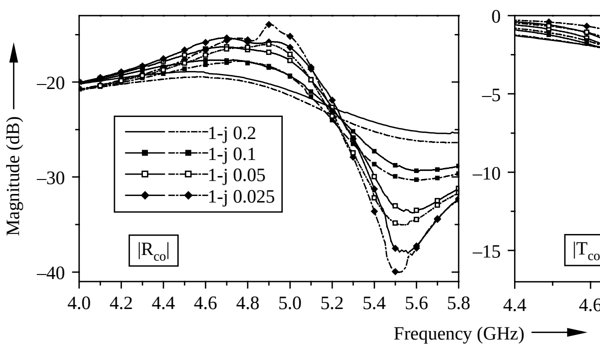

Note: Solid line: scattering approach, dashed-dotted line: CM theory

Figure 13.
Scattering parameters for $\psi = 90°$, $\psi_p = d_m$ and different embedding dielectric spheres (marked by their permittivity)

As expected, the agreement between the two approaches improves with increasing loss. If, in turn, one reduces the mutual coupling of the inclusions by embedding them randomly in a lossy background material, such as in microwave absorbers (Meiners and Jacob, 2006), CM theory could well be applied to tailor the properties of such arrangements (Reinert *et al.*, 2001).

6. Conclusion

Periodic and random layers of small metal helices are investigated. Thereby, periodic boundaries are also applied for random layers, but in conjunction with an averaging hypothesis. The randomness is controlled by a linear parameter used to set a maximum angle between the periodic and actual helix orientations. This exemplary type of variation is studied in view of convergence aspects. Amongst others, it turns out that few helices in the range of 40 per unit cell are convenient to render the statistics. For layers with an appreciable randomness, it is possible to restrict the analysis to dipole interactions. Classical mixing theories, such as from CM can be applied if mutual particle coupling is weak.

References

Berremann, D.W. (1972), "Optics in stratified and anisotropic media: 4×4-matrix formulation", *J. Opt. Soc. Am.*, Vol. 62, pp. 502-10.

Chen, X., Grzegorczyk, T.M., Wu, B., Pacheco, J. Jr. and Kong, J.A. (2004), "Robust method to retrieve the constitutive effective parameters of metamaterials", *Phys. Rev. E.*, Vol. 70, p. 016608.

Ding, K.H., Mandt, C.E., Tsang, L. and Kong, J.A. (1992), "Monte carlo simulations of pair distribution functions of dense discrete random media with multiple sizes of particles", *J. Electromagn. Waves and Appl.*, Vol. 6, pp. 1015-30.

Guérin, F., Bannelier, P., Labeyrie, M., Ganne, J.-P. and Guillon, P. (1995), "Scattering of electromagnetic waves by helices and application to the modelling of chiral composites: II Maxwell Garnett treatment", *J. Phys D.: Appl. Phys.*, Vol. 28, pp. 643-56.

Lindell, I.V., Sihvola, A.H., Tretyakov, S.A. and Viitanen, A.J. (1994), *Electromagnetic Waves in Chiral and Bi-isotropic Media*, Artech House, London.

Meiners, C. and Jacob, A.F. (2006), "Full-wave analysis of composite absorbing layers", *Proceedings of the 36th European Microwave Conference, Manchester, UK*, pp. 1011-4.

Meiners, C. and Jacob, A.F. (2008), "Numerical and experimental parameter study of helix layers", *IEEE Trans. Antennas Propagat.*, Vol. 56 No. 5, pp. 1321-8.

Meiners, C., Richter, M.D. and Jacob, A.F. (2008), "Higher-order multipole model of a thin-wire helix", *IEEE Trans. Antennas Propagat.*, Vol. 56 No. 10, pp. 3166-72.

Reinert, J., Psilopoulos, J., Grubert, J. and Jacob, A.F. (2001), "On the potential of graded-chiral Dallenbach absorbers", *Microwave Opt. Technol. Letters*, Vol. 30, pp. 254-7.

Sihvola, A.H. (1999), *Mixing Formulae and Applications,* Electromagnetic Waves Series, Vol. 47, IEE Publishers, London.

Smith, D.R., Schultz, S. and Marcoš and Soukoulis, C.M. (2002), "Determination of effective permittivity and permeability of metamaterials from reflection and transmission coefficients", *Phys. Rev. B.*, Vol. 65, p. 195104.

Whites, K.W. (1995), "Full wave computation of constitutive parameters for lossless composite chiral materials", *IEEE Trans. Antennas Propagat.*, Vol. 43 No. 4, pp. 376-84.

About the authors

Christian Meiners was born in Lohne, Germany, in 1977. He received the Diploma in Electrical Engineering from the Technische Universität Braunschweig in 2002 and the PhD in Electrical Engineering from the Technische Universität Hamburg-Harburg in 2009. His research interests include electromagnetic theory, the modeling of wave propagation in complex materials, numerical methods, and signal processing techniques. Christian Meiners is the corresponding author and can be contacted at: christian.meiners@tuhh.de

Arne F. Jacob was born in Braunschweig, Germany, in 1954. He received the Diploma in Electrical Engineering and the PhD in Electrical Engineering from the Technische Universität in Braunschweig in 1979 and 1986, respectively. From 1986 to 1988, he was a Fellow with the Centre Européen pour la Recherche Nucléaire (CERN) (the European Laboratory for Particle Physics), Geneva, Switzerland. He then spent three years with the Accelerator and Fusion Research Division, Lawrence Berkeley Laboratory, University of California at Berkeley, USA. In 1990, he joined the Institut für Hochfrequenztechnik, Technische Universität Braunschweig, as a Professor. Since 2004, he has been a Professor at the Technische Universität Hamburg-Harburg, Hamburg, Germany. His current research interests include the design, packaging, and application of integrated subsystems up to millimeter frequencies, and the characterization of complex materials.